Physics Letters B 673 (2009) 5–8

Contents lists available at ScienceDirect

Physics Letters B

www.elsevier.com/locate/physletb

Hard bremsstrahlung in the $pp \to pp\gamma$ reaction

A. Johansson [a], C. Wilkin [b,*]

[a] Division of Nuclear and Particle Physics, Uppsala University, Box 516, S-751 20 Uppsala, Sweden
[b] Physics and Astronomy Department, UCL, London, WC1E 6BT, UK

ARTICLE INFO

Article history:
Received 22 December 2008
Received in revised form 29 January 2009
Accepted 29 January 2009
Available online 4 February 2009
Editor: D.F. Geesaman

PACS:
25.40.Ep
25.20.-x
13.60.-r

Keywords:
Hard bremsstrahlung
Proton–proton collisions
Diproton

ABSTRACT

The $pp \to pp\gamma$ reaction has been measured at a beam energy of 310 MeV by detecting both final protons in the PROMICE-WASA facility and identifying a missing-mass peak. For those events where the pp excitation is less than 3 MeV, the final diproton is almost purely in the ${}^1S_0$ state and, under these conditions, there is complete coverage in the photon c.m. angle θ_γ. The linear behaviour observed in $\cos^2\theta_\gamma$ shows that there is almost no influence of an E2 multipole at this energy, though the E1 and M2 must be rather similar in size.

Hard bremsstrahlung produced through the two-body $pn \to d\gamma$ reaction has been studied for many years in either the direct or inverse (photoabsorption) reaction. Much less is known about the other *elementary* case of $pp \to \{pp\}_s\gamma$, where the $\{pp\}_s$ system is at very low excitation energy E_{pp}, such that the final diproton is in the spin-singlet S-wave, *i.e.* in the ${}^1S_0$ state. The selection rules in the two cases are very different; the production of an intermediate $\Delta(1232)$ isobar is very important for the np reaction whereas for the pp case the dominant $\Delta(1232)N$ intermediate contribution is forbidden [1]. A comparison of $pn \to d\gamma$ and $pp \to \{pp\}_s\gamma$ might therefore cast light on these high energy bremsstrahlung processes.

Recent results on $pp \to \{pp\}_s\gamma$ have been published by the COSY-ANKE Collaboration at beam energies of $T_p = 353$, 500, and 550 MeV [2]. The events were selected by demanding that the excitation energy of the two observed protons was less than 3 MeV. Although the coverage was limited to near-forward proton angles, corresponding to $\cos\theta_\gamma > 0.95$, the data seemed to indicate a forward dip, especially at the two higher energies. The observed distribution in E_{pp} was consistent with that expected from a final state interaction (*fsi*) in the ${}^1S_0$ channel and the angular distribution in the pp rest frame was also isotropic, as required for an S wave.

Most of the earlier experiments were carried out using pairs of counters placed on either side of the beam line and, as a consequence, they had little or no acceptance at small E_{pp} [3]. One exception was the COSY-TOF work at 300 MeV [4], but comparatively few events were obtained at low E_{pp} and it was not possible to construct an angular distribution for such a selection.

Attempts have been made to study the problem by looking at the photoabsorption on ^{3}He leading to two fast protons and a "spectator" neutron, ${}^3\text{He}(\gamma,2p)n$ [5–7]. Interpreting these data in terms of photoabsorption on a bound diproton, it was claimed that, at energies corresponding to $T_p \approx 400$–600 MeV, the reaction was dominated by an E2 transition. Unfortunately, the fraction of events associated with quasifree absorption was only about 5% of the total [5] and so there could be significant contamination arising from the much larger absorption on quasi-deuteron pairs in the ^{3}He nucleus. A further cause for caution is that there is also a small fraction of P-wave spin-triplet pp pairs in ^{3}He [8].

The possible observables in $pp \to \{pp\}_s\gamma$, and their relation to the production amplitudes, have been very clearly spelled out in Ref. [9]. Taking just the three lowest multipoles, and neglecting possible contributions from high initial partial waves, the differential cross section should be of the form:

$$\frac{d\sigma}{d\Omega} = \frac{3}{8\pi}\left[|\mathrm{E1}+\mathrm{M2}|^2 + 3|\mathrm{E1}-\mathrm{M2}|^2\cos^2\theta_\gamma + 10|\mathrm{E2}|^2\sin^2\theta_\gamma\cos^2\theta_\gamma\right], \qquad (1)$$

* Corresponding author.
E-mail address: cw@hep.ucl.ac.uk (C. Wilkin).

0370-2693 © 2009 Elsevier B.V. Open access under CC BY license.
doi:10.1016/j.physletb.2009.01.069

where $|\mathrm{E1}|^2$, $|\mathrm{M2}|^2$, and $|\mathrm{E2}|^2$ represent the contributions of the individual multipoles to the integrated cross section. It is clear from this that, in the absence of E2, the differential cross section should be linear in $\cos^2\theta_\gamma$. However, even in this case, one would require photon polarisation measurements in order to isolate the individual $|\mathrm{E1}|^2$ and $|\mathrm{M2}|^2$ terms. Furthermore, since $|\mathrm{E1}-\mathrm{M2}|^2$ cannot be negative, the cross section should be forward-peaked. Deviations from linearity would be a sign of the influence of an E2 multipole.

Estimates within dynamical models [10,11] suggest that the E2 term should be quite large in the $T_p > 200$ MeV region and, if this is the case, the cross section could exhibit a forward dip, as indicated by the higher energy COSY-ANKE data [2]. To investigate fully this one needs $pp \to \{pp\}_s\gamma$ data over a much wider angular interval and this has proved possible to obtain at 310 MeV by using the PROMICE-WASA facility [12] situated at the CELSIUS storage ring [13] of the The Svedberg Laboratory.

The $pp \to pp\gamma$ data reported here were collected simultaneously with those for $pp \to pp\pi^0$ [14]. The detector assembly and the experimental techniques were therefore identical and the analyses of the data differ only in minor details, so that we can here be brief.

An internal gas-jet hydrogen target was used in conjunction with the stored proton beam. By operating the electron cooler throughout the experiment, the background was reduced and the counting rate increased due to the larger beam-target overlap. The integrated luminosity of 340 ± 35 nb^{-1} was found by comparing the numbers of simultaneously measured elastically scattered proton events with world cross section data, as described in Ref. [14].

Protons from π^0 production have a maximum laboratory polar angle of around 18°. The exact value depends sensitively upon the energy of the stored proton beam and its measurement determined that $T_p = 309.7 \pm 0.3$ MeV.

For the bremsstrahlung study reported here, only the protons in the final state were used, even though the detector system was also capable of measuring photons. After exiting the scattering chamber, the protons passed through a forward window counter (FWC), a tracker, a forward trigger hodoscope (FTH) and usually stopped in a forward range hodoscope (FRH). The four-quadrant scintillator of the FWC eliminated most of the beam halo background but using this meant that the coincident protons had to appear in different quadrants in order to be detected.

Angular information for the protons was extracted from the FTH and most precisely from the tracker. The system covered a range in proton polar angles $3° < \theta_p < 22°$. Due to a small misalignment of the detector system with respect to the beam axis, there was a small dependence on the azimuthal angle, which was taken into account in the Monte Carlo analysis.

In order to ensure particle identification, it was further required that both protons of an accepted event penetrated at least into the second layer of the FTH, consisting of 24 spiral scintillator segments. This meant that the minimum proton energy was 39 MeV. There was no high energy limit since all the relevant protons stopped in the second FRH scintillator or earlier.

As described in detail in Ref. [14], the energy associated with a proton track was obtained from a combination of the calculated angle-dependent range up to the entrance of the stopping scintillator and the measured light output of that detector. A few of the protons stopped in the dead region between scintillators and in such cases they were assumed to have an energy corresponding to the midpoint of the dead layer.

A time signal was extracted for each proton from the first layer of the FTH. After calibrating the individual detectors and correcting for the times of flight, a time-difference Δt spectrum was obtained with a FWHM of 0.9 ns. Thus, by accepting only events with $|\Delta t| <$ 1.8 ns, the number of accidental coincidences was kept to of the order of one percent.

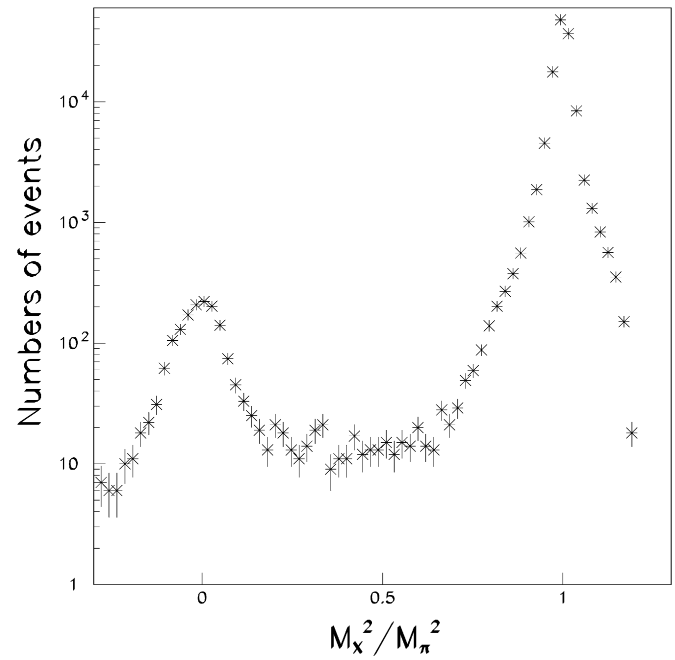

Fig. 1. Distribution in missing-mass squared of the $pp \to \{pp\}_s X$ reaction for events with $E_{pp} < 3$ MeV presented in units of the neutral pion mass. Clear peaks are seen corresponding to the $pp \to \{pp\}_s\pi^0$ and $pp \to \{pp\}_s\gamma$ reactions sitting on a slowly varying background.

The raw data were reduced to be stored in intermediate files and these were already used to produce very preliminary results [15]. Information was included on particle identity, azimuthal and polar angles, energies, timing and energy loss in the last detector of each track. About 60,000 events were seen in the missing-mass peak attributed to the $pp\gamma$ final state.

In a first step of the analysis, events were selected where the excitation energy in the pp rest system, E_{pp}, was less than 3 MeV. The square of the missing mass was evaluated for these events and the resulting spectrum is shown in Fig. 1. The data show two clear peaks corresponding to the production of $\{pp\}_s\pi^0$ and $\{pp\}_s\gamma$ final states. The γ-peak, of width $\sigma(M_X^2)_\gamma \approx 0.06M_{\pi^0}^2$, contains in total about 1450 events. This is sitting on a smoothly varying background which is at about the 10% level. To a good approximation, this can be taken into account by keeping all events where $|M_X^2/M_{\pi^0}^2| < 0.137$ and this criterium was applied in all the angular bins. However, the background was larger for slow protons and, rather than attempting to correct for this, data were only used with $\cos\theta_\gamma < 0.8$. Due to the forward–backward symmetry of the cross section, this did not result in any reduction in the angular coverage.

In order to convert the observed number of events for given E_{pp} and θ_γ values into cross sections, one needs to know the detector acceptance as a function of these parameters. This was achieved by Monte Carlo techniques, where the only deviation from phase space was assumed to come from the pp final-state-interaction function discussed below. The detector system was described in great geometric detail, with the simulated and experimental events being required to pass the same tests. The acceptance was found to be quite large, in most cases lying between 20% and 30%.

The $pp \to \{pp\}_s\gamma$ differential cross section is shown summed over all angles in Fig. 2 as a function of the diproton excitation energy. The shoulder at small E_{pp} is a clear enhancement compared to phase space, which varies like $\sqrt{E_{pp}}$ in this region. This is caused by the S-wave final state interaction.

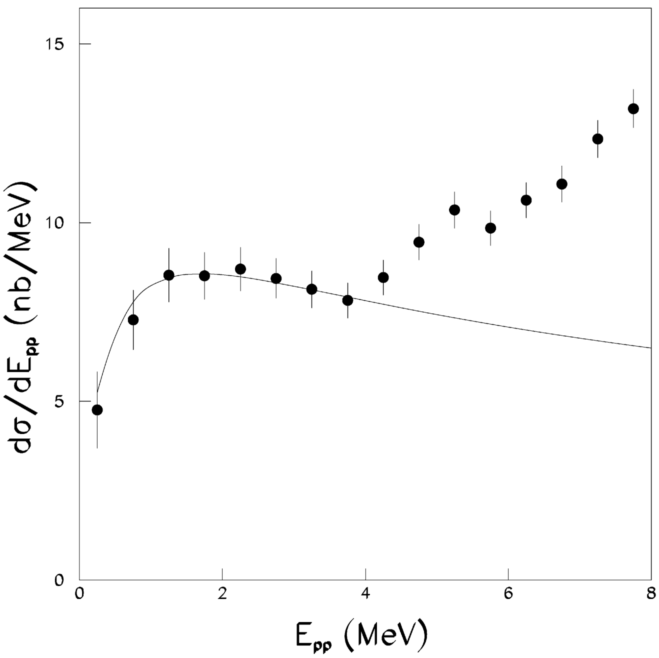

Fig. 2. Differential cross section for all $pp \to \{pp\}_s\gamma$ events in terms of the excitation energy in the diproton. The simulation of the shape of the S-wave *fsi* enhancement is based on Eq. (2).

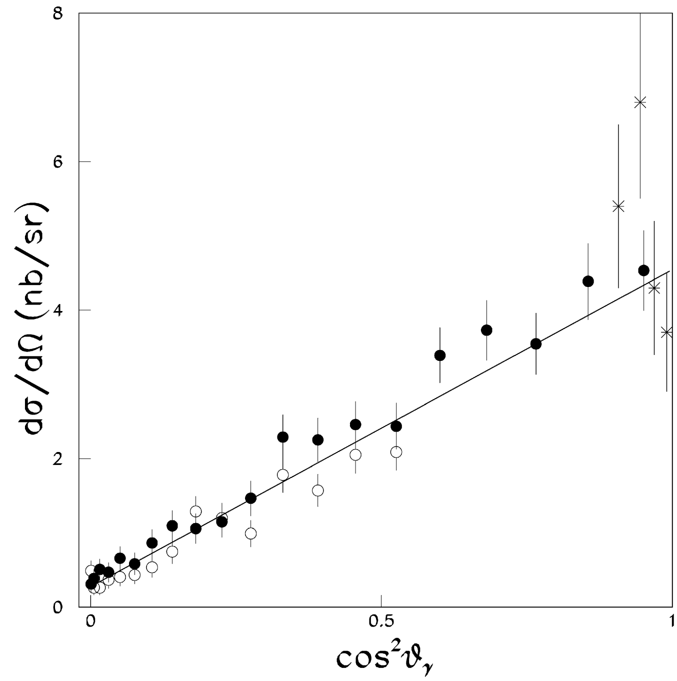

Fig. 3. Differential cross section for the $pp \to \{pp\}_s\gamma$ reaction for $E_{pp} < 3$ MeV as a function of $\cos^2\theta_\gamma$. The present data at 310 MeV are shown by closed circles for the backward photon hemisphere and open ones for the forward. The COSY-ANKE results at 353 MeV [2] are denoted by crosses. The line represents a linear fit to both sets of CELSIUS points.

In the early Uppsala work on π^0 production [16], the effect was evaluated in terms of the square of the $^1S_0$ pp wave function at its peak ($r = 1$ fm), divided by the corresponding plane wave. In the case of the Paris wave function [17] the enhancement factor may be parameterised for low E_{pp} in the form

$$F_{fsi}(q) = \frac{1 + 2.80q^2 + 20.28q^4 - 15.94q^6}{(1 + 51.02q^2)(1 + 14.36q^2)} \frac{m\pi\alpha/q}{\exp(m\pi\alpha/q) - 1}, \qquad (2)$$

where m is the proton mass, α the fine structure constant, and the pp relative momentum $q = \sqrt{mE_{pp}}$ is measured in fm^{-1}. It should be noted that no hard evidence is to be found for the pp *fsi* in the COSY-TOF data [4].

The enhancement factor of Eq. (2) describes well the shape of the differential cross section of Fig. 2 up to about 4 MeV, when it seems that P and higher waves start to become more important. There is therefore likely to be very little contamination to the S-wave if we only retain data for $E_{pp} < 3$ MeV. The direction of the pp relative momentum vector is hard to determine with precision for such small E_{pp} but, just as for the COSY-ANKE experiment [2], the distribution in this vector is consistent with isotropy.

The angular distributions in both hemispheres are shown in Fig. 3 in terms of $\cos^2\theta_\gamma$. These two data sets are fairly consistent within the error bars, which reflects the good description of the apparatus during the data analysis. Also shown on this figure are the four points from the COSY-ANKE Collaboration [2]. Although these were obtained at the slightly higher energy of 353 MeV, they fall very close to our results.

Fitting the CELSIUS angular distribution with the multipoles present in Eq. (1) leads to

$$|\text{E1} + \text{M2}|^2 = 2.3 \pm 0.5 \pm 0.3 \text{ nb},$$
$$|\text{E1} - \text{M2}|^2 = 11.9 \pm 0.6 \pm 0.5 \text{ nb},$$
$$|\text{E2}|^2 < 0.2 \text{ nb}, \qquad (3)$$

where the first error is systematic, reflecting the slight differences in results in the forward and backward hemispheres apparent in Fig. 3, and the second is statistical. There are in addition overall systematic uncertainties of about 15% that arise principally from the luminosity determination, acceptance evaluation, and background subtraction. The statistically best fit is obtained with the negative value of $|\text{E2}|^2 = -1.0 \pm 0.6$ nb and so only an upper limit is quoted in Eq. (3) at the one standard deviation level.

Although the individual contributions of the E1 and M2 multipoles cannot be extracted from the data, it is clear from these results that at 310 MeV $|\text{E1}|^2$ and $|\text{M2}|^2$ must be rather similar in size, as indicated by theoretical estimates [10]. If we define the ratio $\text{M2}/\text{E1} = -re^{i\phi}$, the data require that the phase $|\phi| < 50°$ and the magnitude $0.36 < r < 2.8$, though this full range is only allowed if ϕ is very small. A more rigorous bound might be established if the phase were constrained by using the Watson theorem. It is important to stress that there is no sign at all of any significant E2 signal that was also predicted to be very large [10] and further theoretical work in this area would be most welcome.

On the other hand, there is evidence from the forward dip that there must be large contributions from higher multipoles at 500 and 550 MeV [2] and these might reflect in some form the influence of the $\Delta(1232)$ isobar. The situation could be clarified through measurements of proton analysing powers and spin correlations [9] and this might be possible at COSY [18].

In summary, we have measured the $pp \to \{pp\}_s\gamma$ differential cross section over the full angular range for low excitation energies in the pp final state. The behaviour in E_{pp} is consistent with the belief that below 3 MeV the two protons are almost entirely in the $^1S_0$ state. The photon angular distribution shows that the E1 and M2 multipoles are comparable in size but that, contrary to theoretical expectation, E2 is quite small. The acceptance of the PROMICE-WASA apparatus is very good for small E_{pp} but the proton angular limitation to 22° in the laboratory system is equivalent to a maximum possible E_{pp} of 42 MeV. An analysis up to this limit will be reported on at a later stage.

Acknowledgements

We are very grateful to the TSL/ISV personnel for their participation during the course of this work. The PROMICE-WASA Collaboration is acknowledged for the essential contributions described in Ref. [14]. We are particularly grateful to Jozef Złomańczuk, who constructed the important intermediate data files. Discussions and correspondence with K. Nakayama on the theoretical implications of the $pp \to \{pp\}_s\gamma$ reaction were much appreciated. This work was supported by the European Community under the "Structuring the European Research Area" Specific Programme Research Infrastructures Action (Hadron Physics, contact number RII3-cT-204-506078), and by the Swedish Research Council.

References

[1] J.M. Laget, Nucl. Phys. A 497 (1989) 391.
[2] V.I. Komarov, et al., Phys. Rev. Lett. 101 (2008) 102501.
[3] B.M.K. Nefkens, et al., Phys. Rev. C 19 (1979) 877;
K. Michaelian, et al., Phys. Rev. D 41 (1990) 2689;
B.V. Przewoski, et al., Phys. Rev. C 45 (1992) 2001;
K. Yasuda, et al., Phys. Rev. Lett. 82 (1999) 4775;
M. Mahjour-Shafiei, et al., Phys. Rev. C 70 (2004) 024004.
[4] R. Bilger, et al., Phys. Lett. B 429 (1998) 195.
[5] T. Emura, et al., Phys. Rev. Lett. 73 (1994) 404.
[6] S. Niccolai, et al., Phys. Rev. C 70 (2004) 064003.
[7] G. Audit, et al., Phys. Lett. B 312 (1993) 57.
[8] R.B. Wiringa, R. Schiavilla, S.C. Pieper, J. Carlson, Phys. Rev. C 78 (2008) 021001.
[9] P. Wilhelm, J.A. Niskanen, H. Arenhövel, Nucl. Phys. A 597 (1996) 613.
[10] P. Wilhelm, J.A. Niskanen, H. Arenhövel, Phys. Rev. C 51 (1995) 2841;
P. Wilhelm, J.A. Niskanen, H. Arenhövel, Phys. Rev. Lett. 74 (1995) 1034.
[11] V. Hermann, J. Speth, K. Nakayama, Phys. Rev. C 43 (1991) 394;
K. Nakayama, private communication.
[12] H. Calén, et al., Nucl. Instrum. Methods A 379 (1996) 57.
[13] C. Ekström, et al., Phys. Scr. T 22 (1988) 256.
[14] R. Bilger, et al., Nucl. Phys. A 693 (2001) 633.
[15] J. Złomańczuk, A. Johansson, WASA Collaboration, Nucl. Phys. A 631 (1998) 622.
[16] J. Złomańczuk, et al., Phys. Lett. B 436 (1998) 251.
[17] M. Lacombe, et al., Phys. Rev. C 21 (1980) 861.
[18] A. Kulikov, et al., COSY proposal #158, http://www.fz-juelich.de/ikp/anke/en/proposals.shtml.